analytical chemistry

Article

pubs.acs.org/ac

# Aptamer-Based Label-Free Impedimetric Biosensor for Detection of Progesterone

Gastón Contreras Jiménez,[†] Shimaa Eissa,[†,‡] Andy Ng,[‡] Hani Alhadrami,[§] Mohammed Zourob,[∥,⊥] and Mohamed Siaj*[,†]

[†]Département de Chimie et Biochimie, Université du Québec à Montréal, Montréal, Québec H3C 3P8, Canada

[‡]Centre Énergie Matériaux Télécommunications, Institut National de la Recherche Scientifique, Varennes, Québec J3X 1S2 Canada

[§]Faculty of Applied Medical Sciences, King Abdulaziz University, Post Office Box 80402, Jeddah 21589, Kingdom of Saudi Arabia

[∥]Center of Biomedical Engineering, School of Engineering, Cranfield University, Cranfield, Bedfordshire MK43 0AL, United Kingdom

[⊥]Chemistry Department, Alfaisal University, Al Zahrawi Street, Al Maather, Al Takhassusi Road, Riyadh 11533, Kingdom of Saudi Arabia

Supporting Information

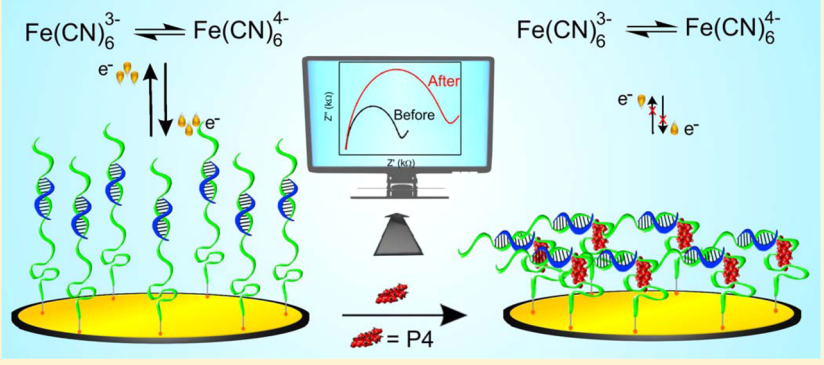


**ABSTRACT:** Rising progesterone (P4) levels in humans due to its overconsumption through hormonal therapy, food products, or drinking water can lead to many negative health effects. Thus, the simple and accurate assessment of P4 in both environmental and clinical samples is highly important to protect public health. In this work, we present the selection, identification, and characterization of ssDNA aptamers with high binding affinity to P4. The aptamers were selected in vitro from a single-stranded DNA library of $1.8 \times 10^{15}$ oligonucleotides showing dissociation constants ($K_D$) in the low nanomolar range. The dissociation constant of the best aptamer, designated as P4G13, was estimated to be 17 nM by electrochemical impedance spectroscopy (EIS) as well as fluorometric assay. Moreover, the aptamer P4G13 did not show cross-reactivity to analogues similar to progesterone such as 17$\beta$-estradiol (E2) and norethisterone (NET). An impedimetric aptasensor for progesterone was then fabricated based on the conformational change of P4G13 aptamer, immobilized on the gold electrode by self-assembly, upon binding to P4, which results in an increase in electron transfer resistance. Aptamer−complementary DNA (cDNA) oligonucleotides were tested to maximize the signal gain of the aptasensor after binding with progesterone. Significant signal enhancement was observed when the aptamer hybridized with a short complementary sequence at specific site was used instead of pure aptamer. This signal gain is likely due to the more significant conformational change of the aptamer−cDNA than the pure aptamer upon binding with P4, as confirmed by circular dichroism (CD) spectroscopy. The developed aptasensor exhibited a linear range for concentrations of P4 from 10 to 60 ng/mL with a detection limit of 0.90 ng/mL. Moreover, the aptasensor was applied in spiked tap water samples and showed good recovery percentages. The new selected progesterone aptamers can be exploited in further biosensing applications for environmental, clinical, and medical diagnostic purposes.

Endocrine-disrupting chemicals (EDCs) are substances that may exist in our drinking water and food products that interfere with hormones biosynthesis, metabolism, or action resulting in a deviation from normal homeostatic control or reproduction.[1] The presence of these EDCs above or below a certain threshold may cause adverse effects in wildlife as well as humans by interfering with the normal function of the endocrine system. Progesterone (P4) is a 21-carbon steroid hormone secreted mainly by the corpus luteum, associated with the establishment and maintenance of mammalian pregnancy

**Received:** September 28, 2014
**Accepted:** December 8, 2014
**Published:** December 8, 2014






DOI: 10.1021/ac503639s
*Anal. Chem.* 2015, 87, 1075−1082

and essentially required for growth and development of the animal. Progesterone is used as menopausal hormone therapy, to regulate abnormal menstrual cycles, and as hormone replacement therapy for the treatment of gender dysphoria.[2,3] However, high amounts of P4 in women may cause side effects such as breast tenderness, headache, upset stomach, constipation, diarrhea, vomiting, tiredness, body pain, irritability, mood swings, excessive worrying, sneezing, runny nose, cough, vaginal discharge, and urination problems.[4] Excess consumption of high P4 in milk may result in breast and lung cancers.[5] High levels of P4 in males may also provoke a negative effect on gonadotropin releasing hormone (GnRH) secretion,[6] which may lead to a decrease of testosterone secretion and affect male behavior.[7] When high doses of this progestogen are consumed by humans, usually the body just absorbs low amounts and the rest is passed as waste to sewage water and may affect the environment. Therefore, accurate monitoring of P4 concentration in both environmental and clinical samples is highly important. Several methods are currently employed for P4 detection. Instrumental analysis methods such as HPLC, LC/MS, or GC/MS are very sensitive with a limit of detection ranging from 0.01 to 0.21 ng/L.[8,9] However, these methods are usually costly and time-consuming and require highly trained personnel to perform, and thus they are not suitable for field applications. Immunological methods such as enzyme-linked immunosorbent assay (ELISA) and radioimmunoassay (RIA) are also currently utilized for P4 detection.[10,11] However, RIA requires specialized and expensive equipment to handle the radioactive and hazardous materials, which brings environmental protection concerns, and ELISA kits are still expensive, time-consuming, and require multiple steps.

Recently, immunosensors have been shown as a good alternative to these traditional analytical and immunological methods for P4 detection. Several optical immunosensors for P4 detection based on surface plasmon resonance,[12] total internal reflectance fluorescence,[13,14] and integrated optical grating coupler[15] have been reported to show good sensitivity. Moreover, electrochemical immunosensors have been also reported based on amperometry,[16,17] differential pulse voltammetry,[18] and chronoamperometry[19] detection, showing lower cost and more simplicity and capability of miniaturization than optical assays. Nevertheless, a major weakness of these immunosensors is the use of antibodies as biorecognition receptor. The production of antibodies is highly costly and requires the use of experimental animals, which raises ethical concerns.[20,21] Moreover, antibodies targeting similar molecules usually suffer from cross-reactivities and requires special storage and handling conditions.

Recently, aptamers as bioreceptors have emerged as a good alternative to antibodies in the development of biosensor devices[22,23] because of their high stability and easier chemical synthesis with very low cost. Aptamers are small single-stranded DNA (ssDNA) or RNA sequences (oligonucleotides of ∼100 nucleotides or less) that fold into a unique 3D structure due to intramolecular interactions between nucleotides. Because of such unique structures, aptamers can bind with high affinity to a specific analyte by intermolecular interactions such as hydrogen bonds and van der Waals forces.[24,25] In the last two decades, many aptamers have been selected against various analytes such as bacteria, viruses,[26] proteins,[27] and small molecules[28−31] and even ions such as $Hg^{2+}$,[32] with high affinity and specificity. These aptamers have opened the way for fabricating a new generation of biosensor devices with lower cost, greater stability, and much simpler detection strategies than immunosensors. Only a few aptamers targeting hormones have been identified so far, such as 17$\beta$-estradiol,[33] hormone abscisic acid,[34] thyroxine,[35] and vasopressin.[36] In this work, we report for first time the selection and characterization of aptamers that bind progesterone and their application in a biosensing platform. The aptamers were obtained from a diverse random library of $\sim 10^{15}$ ssDNA sequences through in vitro selection procedures. After selection, the affinity, cross-reactivity, and conformational change of the selected aptamer was characterized. Finally, a simple label-free biosensing aptamer-based platform for progesterone detection was developed.

## EXPERIMENTAL SECTION

**Materials, Reagents, and Instrumentation.** All materials, reagents, and instrumentation are described in detail in Supporting Information.

**Progesterone Immobilization on Agarose Beads.** Progesterone was coupled to diaminodipropylamine (DADPA) agarose beads (P4−beads) following the protocol reported previously. Briefly, 11 $\mu$mol of progesterone 3-*O*-carboxymethyloxime (P4 3-O-CMO) was dissolved in 0.5 mLof dimethyl sulfoxide (DMSO) and then mixed with 0.36 mmol of 1-ethyl-3-(3-dimethylaminopropyl)carbodiimide hydrochloride (EDC-HCl) in 1.0 mL of coupling buffer [0.5 M 2-(*N*-morpholino)ethanesulfonic acid (MES) buffer, pH 4.7] to be activated. The activated hormone was immediately added to 2 mL of washed DADPA agarose beads in coupling buffer to react for 3 h by mild shaking at 25 °C in 5.5 mL final volume. Afterward, the beads were washed with 1 M NaCl solution to remove the unreacted P4. Then, the unreacted amine functions on the beads were blocked by incubation in *N*-hydroxysulfosuccinimide (sulfo-NHS)−acetate solution in 1 M carbonate buffer, pH 8.6, and rotation for 1 h, after which the beads were washed extensively with binding buffer and kept at 4 °C. The coupling between DADPA agarose beads and P4 3-O-CMO (P4 immobilization) was confirmed by an ELISA test. Primary anti-P4 3-O-CMO rabbit monoclonal antibody and horseradish peroxidase (HRP)-labeled goat antirabbit IgG secondary polyclonal antibody were used in the assay.

**Random ssDNA Library and Primer Design.** A random ssDNA library of $1.80 \times 10^{15}$ (3 nmol) oligonucleotides was chemically synthesized and purified by polyacrylamide gel electrophoresis (PAGE). The ssDNA library consisted of a central random region of 60 nucleotides flanked by two 18-nucleotide primers at 3′ and 5′ ends. The primers are binding sites for polymerase chain reaction (PCR) amplification of each ssDNA sequence, 5′-ATACCAGCTTATTCAATT-$N_{60}$-AGATAGTAAGTGCAATCT-3′ (96-mer). To facilitate the separation of the desirable ssDNA from double-stranded DNA (dsDNA) symmetric PCR products, the reverse primer was labeled with hexaethylene glycol (HEGL) linker (to block the polymerase extension) followed by a ssDNA tail of 20 dA: labeled reverse primer 5′- poly($dA_{20}$)-HEGL-AGATTGCACTTACTATCT-3′. To quantify separated and recovered ssDNA, the forward primer was labeled with fluorescein isothiocyanate (FITC) fluorophore: labeled forward primer fluorescein-5′-TATACCAGCTTATTCAATT-3′. Unlabeled primers set were specifically used for PCR amplification for cloning step when in vitro selection rounds were completed.

**In Vitro Selection of Progesterone Aptamers.** Five consecutive steps were performed for each round (Scheme 1):


DOI: 10.1021/ac503639s
*Anal. Chem.* 2015, 87, 1075−1082

Scheme 1. Diagram of Systematic Evolution of Ligands by Exponential Enrichment (SELEX) Protocol

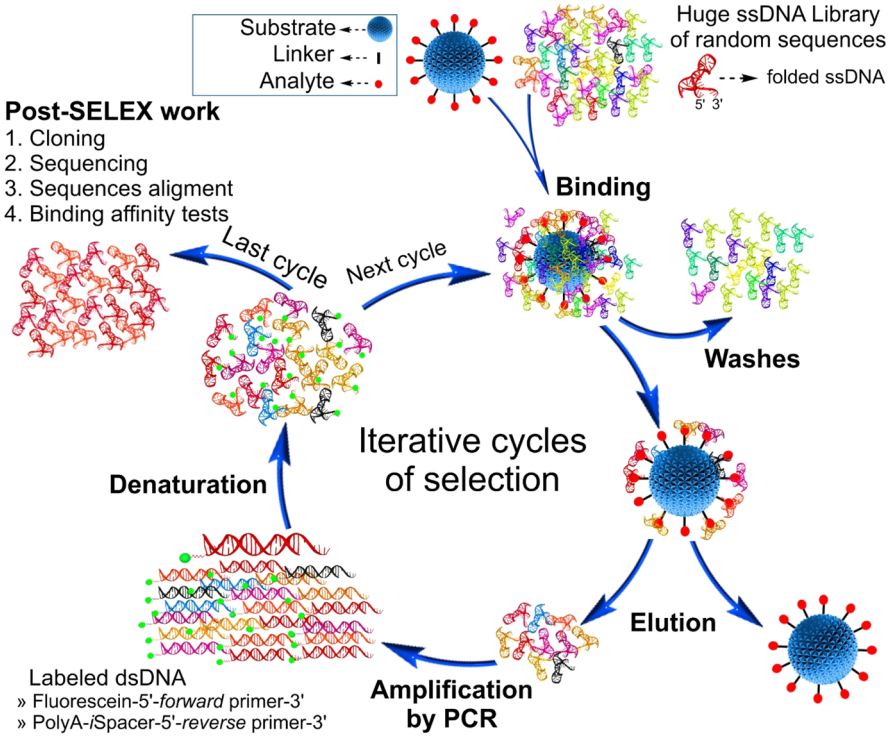


(1) incubation of DNA library with P4−beads, (2) separation of unbound DNA from P4−beads by washing, (3) elution of DNA sequences bound to P4, (4) desalting and PCR amplification of eluted DNA, and (5) denaturation of dsDNA aptamer from PCR products by PAGE. A negative selection cycle was performed in the 11th cycle, and a specific elution (SE) was used to elute the bound ssDNA in the last two cycles. DNA from the last cycle was then cloned and sequenced. All the details of selection and cloning can be found in Supporting Information.

**Electrochemical Measurements.** Cyclic voltammetry (CV) experiments were conducted at a scan rate of 50 or 100 mV/s. Electrochemical impedance spectroscopy (EIS) was recorded over a frequency range from 10 kHz to 0.1 Hz using an alternative voltage with an amplitude of 10 mV, superimposed on a dc potential of 0.23 V (vs Ag/AgCl reference electrode). The impedance data were plotted in the form of complex plane diagram (Nyquist plot) with a sampling rate of 25 points/decade. The obtained spectra were fitted by use of Nova 1.9 software to a modified Randles equivalent circuit. All the EIS and CV measurements were recorded in a 0.01 M phosphate-buffered saline (PBS) solution containing 5 mM $[Fe(CN)_6]^{3-/4-}$ redox pair (1:1 molar ratio).

**Determination of Dissociation Constant $K_D$ by Fluorescence.** Selected ssDNA aptamer sequences were amplified by PCR with the fluorescein-labeled forward primer and the poly-A-labeled reverse primer to allow easy separation of the antiparallel DNA strands and quantification. Each fluorescein-labeled sequence was heated to 90 °C for 10 min, 4 °C for 10 min, and then 25 °C for 5 min. Different amounts of individual sequence (0−300 nM final concentration) were incubated with P4−beads (equivalent to 11.2 pmol of free P4) for 2 h at 25 °C. The mixture was washed and DNA was eluted and quantified as described above. A one-site saturation curve was obtained for each sequence, and their respective $K_D$ values were calculated by nonlinear regression analysis.

**Dissociation Constant Determination by Electrochemical Impedance Spectroscopy.** First, the selected ssDNA aptamer sequences were chemically synthesized without the primer sequences and purified by PAGE. Progesterone molecules were immobilized on a gold electrode surface through an amine-terminated linker as described in detail in Supporting Information. Different concentrations of each sequence (5−300 nM final concentration) were then incubated with the P4-modified electrodes for 40 min at 25 °C (optimized binding time). The electrodes were washed with binding buffer and subjected to EIS measurement. The binding was monitored by measuring the change in charge-transfer resistance ($R_{ct}$) before and after binding with the aptamer. A one-site saturation curve was obtained for the sequences P4G11 and P4G13, and their respective $K_D$ values were also calculated by nonlinear regression analysis.

**Cross-Reactivity Study by Fluorescence Assay.** The cross-reactivities of P4G13 aptamer to NET and E2 as analogues of P4 were tested. Certain amounts of P4G13 sequence were separately incubated with 5 μL of each hormone−beads bath in binding buffer for 1 h at 25 °C with mild shaking; 100 nM of aptamer with P4−beads (equivalent to 11.2 pmol of free P4), 300 nM of aptamer with NET−beads (equivalent to ∼39.5 nmol of free NET), and 300 nM of aptamer with E2−beads (equivalent to ∼69 nmol of free E2).

**Conformation Study of Pure Aptamer and Aptamer-Complementary DNA upon Progesterone Binding .** P4G13 aptamer sequence (5′-GCATCACACACCGATACTCACCCGCCTGATTAACATTAGCCCAC CGCCCACCCCCGCTGC-3′, 60-mer) was partially hybridized with one of its complementary fragment (cDNA2, 5′-TGGGCGGTGG-3′, 10-mer). The hybridization was achieved by mixing equal amounts of the aptamer with


DOI: 10.1021/ac503639s
Anal. Chem. 2015, 87, 1075−1082

cDNA2 in binding buffer and pretreating the solution by incubation at 94 °C for 5 min, then at 47 °C for 5 min, cool down at 4 °C for 10 min, and finally at 25 °C for 5 min. A solution of 1.5 $\mu$M resultant partially double-stranded DNA aptamer (pdsDNA) was incubated separately with 1.5 $\mu$M of P4 free analyte and bisphenol A as control for 1 h. For comparison, 1.5 $\mu$M pure aptamer was also incubated with 1.5 $\mu$M P4. Circular dichroism (CD) spectroscopic measurements were carried out by scanning from 350 to 230 nm the corresponding samples before and after binding to the target analyte. Contributions of binding buffer and analyte spectra to measurements were eliminated by subtraction from the corresponding sample spectra.

**Electrochemical Aptasensor of Progesterone.** Initially, the gold (Au) electrodes were polished with 1, 0.3, and 0.05 $\mu$m particle size alumina slurry ($Al_2O_3$) followed by washing with ultrapure water (18.2 MΩ·cm), ultrasonication for 2 min in water, immersion in piranha solution (3:1 mixture of concentrated $H_2SO_4$ and 30% $H_2O_2$) only for 1 min (to avoid etching and gold oxidation),[37] washing with water, and ultrasonication for 2 min in 100% ethanol. After that, the gold electrode was electrochemically cleaned in 0.5 M $H_2SO_4$ by CV sweeping from 0 to 1.6 V 15 times at 100 mV/s scan rate, followed by washing with ultrapure water. Then the hybridized disulfide-modified HO-$(CH_2)_6$-S-S-$(CH_2)_6$–5′-P4G13-3′ aptamer–cDNA2, prepared under the hybridization conditions described above, was immobilized on the clean Au surface by self-assembly. The Au electrode was incubated in 1 $\mu$M disulfide pdsDNA solution in binding buffer for 16 h and subsequently immersed in 1 $\mu$M 6-mercaptohexanol (MCH) for 30 min in 10 mM PBS, pH 7.4. The modified electrode was then washed thoroughly with binding buffer and immediately used in the electrochemical experiments or kept in binding buffer at 4 °C until later use. For progesterone detection experiments, pdsDNA-modified Au electrodes were incubated in different concentrations of free P4 solutions (0, 10, 20, 30, 40, 50, 60, 70, 80, and 1000 ng/mL) for 40 min, followed by washing the electrode with binding buffer to remove the remained unbound P4, and subjected to EIS measurements. A calibration curve was obtained by plotting the percentage change in charge-transfer resistance upon P4 binding versus P4 concentration.

## RESULTS AND DISCUSSION

**Progesterone Aptamer Selection.** In order to perform SELEX experiments for small-molecule targets, the analyte is usually immobilized on a solid support. We used here a modified form of P4 analyte and performed the coupling to the beads through the external carboxylic modifier to keep all the functional groups of the progesterone molecule available for DNA binding. The carboxylic groups of P4 3-O-CMO were coupled to the terminal amine groups of the DADPA agarose beads via EDC chemistry. The unreacted amine functions on the beads were then blocked with sulfo-NHS–acetate to decrease the possible electrostatic interaction of DNA with amine groups, which can lead to undesirable binding of nonspecific DNA sequences during the selection.[31] A direct ELISA was performed for the P4-coupled beads and negative blocked DADPA beads as a control, with primary anti P4 3-O-CMO rabbit monoclonal antibody as capturing agent and HRP-labeled goat anti-rabbit IgG secondary polyclonal antibody and 3,3′,5,5′-tetramethylbenzidine (TMB) substrate as reporter reagents. A blue color was produced in the P4-coupled beads, indicating the success of the coupling reaction. Aptamer selection against the P4 analyte was carried out through 15 cycles of in vitro selection (or SELEX cycles). The cycles were done as shown in Scheme 1, by incubating a large random library of ssDNA aptamers consisting of $1.80 \times 10^{15}$ sequences in the first round with a constant amount of P4–beads, followed by separation of the bound and unbound DNA. Each selection cycle was monitored by following the bound ssDNA percentage with respect to the total input template ssDNA quantified by fluorescence and UV measurements. As shown in Figure 1, a high ssDNA recovery percentage was observed in

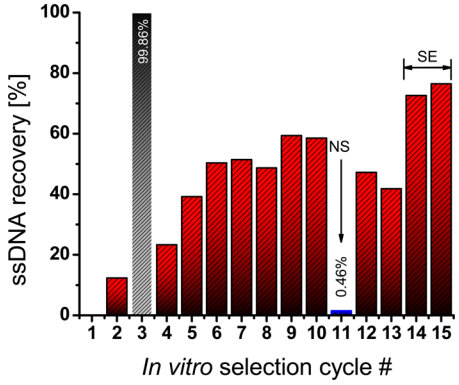


**Figure 1.** Selection of progesterone aptamers: recovery of ssDNA pool after each SELEX cycle. Negative selection (NS) performed by using blank beads, and specific elution (SE) was performed in the two last cycles. The gray column represent the recovery of ssDNA by use of unblocked P4–beads.

the third cycle, which was unexpected to be due to enrichment of P4 bound DNA at this early stage. We presumed that this high recovery was attributed to the strong electrostatic interaction between ssDNA and partially unblocked amine groups on the beads. Therefore, we did further blocking of the beads and significant decrease in the recovery was observed in the subsequent selection cycle, which confirmed the crucial role of the blocking step. We then observed a gradual increase in DNA recovery until the tenth cycle, after which a negative selection (NS) cycle was performed to remove the nonspecifically bound aptamers from the beads matrix. A high amount of ssDNA was retained onto the blank beads, whereas a low amount of DNA was found to be specific to the P4 analyte. However, a significant increase in the DNA recovery was observed again in the next cycle after NS, which indicates the specificity of this low amount of washed ssDNA for P4. In order to increase the stringency of selection and recover the most specific DNA for free P4, specific elution was used in the last two cycles. Due to the low solubility of P4 in water (16.8 mg/L at 25 °C),[38] a saturated solution of P4 was used for the specific elution step by dissolving 1.0 mg in 10 mL of binding buffer. At the 15th SELEX cycle when the ssDNA recovery reached a plateau, SELEX was stopped and the resultant ssDNA pool was cloned and sequenced. A total of 19 aptamers were isolated, identified, aligned, and grouped into eight families on the basis of their common motifs (see Table S1 in Supporting Information).

**Characterization of Selected Aptamers.** The binding affinity of representative ssDNA aptamers to P4 from different families was individually tested by fluorescence assay and their dissociation constants were calculated by nonlinear regression


DOI: 10.1021/ac503639s
Anal. Chem. 2015, 87, 1075–1082

**Table 1. Aptamer Sequences for Progesterone (P4)[a]**

| label | aptamer sequence | $K_D$ (nM) fluorescence | $K_D$ (nM) EIS |
|---|---|---|---|
| P4G11 | CAACGATCGTACCACAGTACCCACCCACCAGCCCCAACATCATGCCCATGCGTCGGTGTG | 15.14 ± 3.75 | 12.58 ± 1.39 |
| P4G06 | CACGCACACAACAGCCAATAATGTATAACGCTGTCCACTGTGTGGTGTCCCCCGCGTCG | 28.66 ± 12.20 | |
| P4G13 | GCATCACACACCGATACTCACCCGCCTGATTAACATTAGCCCACCGCCCACCCCCGCTGC | 35.23 ± 8.30 | 16.81 ± 3.12 |
| P4G04 | GGCACGGCAAAGGGGTACAGCCTACCGAACCGTGGCTGTAAGGGTGGTTGTGGTGTG | 133.30 ± 40.51 | |
| P4G03 | CACACACGCAGCAAGGTCGTCGATACAAAACGTATCGACCCGTCACAGACTGCCCCGGGT | 9.63 ± 3.12 | |

[a] $K_D$ values were determined by fluorescence and EIS measurements. Sequence alignment can be seen in Supporting Information, Table S1.

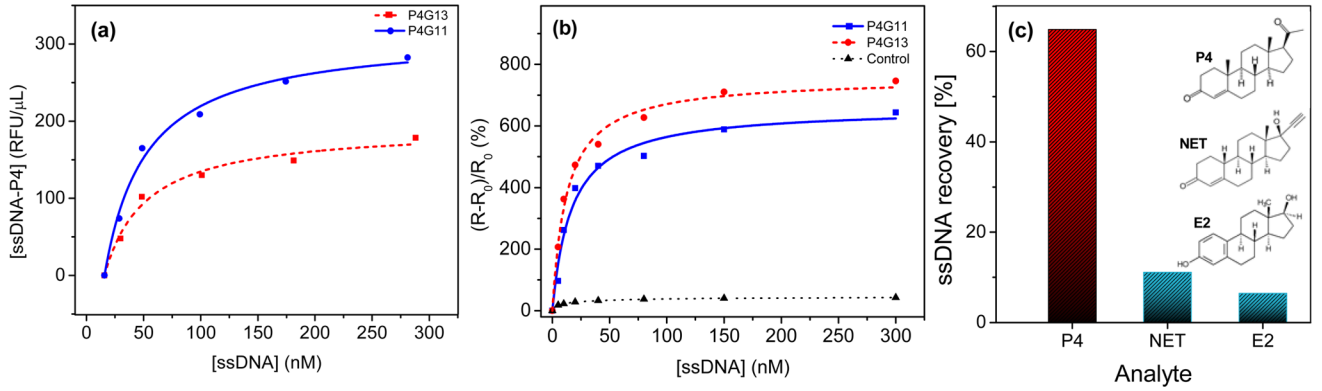


**Figure 2.** Binding affinity assays between ssDNA aptamers and progesterone (P4). Saturation curves were obtained (a) by fluorescence measurements, by plotting the concentration of the complex formed by the binding between ssDNA aptamer and P4 analyte ([ssDNA−P4]) as a function of unbound ssDNA concentration ([ssDNA] = $x$), and (b) by EIS measurements, by plotting the percentage of charge-transfer resistance ($R_{ct}$) value as a function of initial ssDNA aptamer concentration (by considering that $[ssDNA]_0 \gg [ssDNA]$). $B_{max1}$ and $B_{max2}$ are the corresponding total binding sites in each $K_D$ determination. $K_D$ values were determined by nonlinear regression analysis. (c) Cross-reactivity tests of P4G13 aptamer to 17$\beta$-estradiol (E2) and norethisterone (NET).

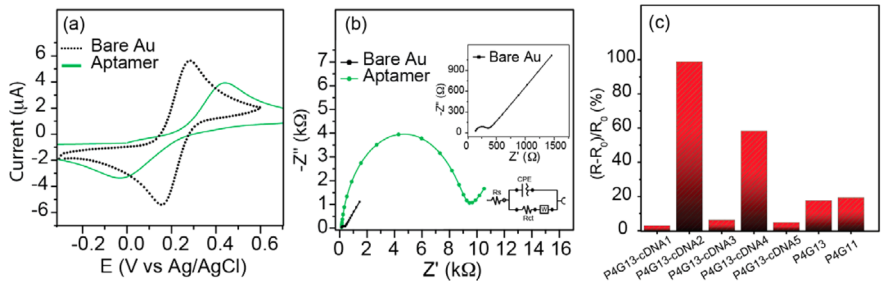


**Figure 3.** (a) Cyclic voltammograms at scan rate 100 mV/s and (b) EIS Nyquist plots recorded in 5 mM $[Fe(CN)_6]^{4-/3-}$ redox couple in 10 mM PBS of bare gold and after the formation of self-assembled monolayer (SAM) of the aptamer. (c) Comparison of aptasensor response, $R - R_0)/R_0$, after saturation point achieved by the different SAM biosensing platforms using different aptameric arrangements.

analysis. As shown in Table 1, all the tested aptamers exhibited $K_D$ values in the low nanomolar range, which implies high affinity for the P4 analyte. Figure 2a shows the plot of saturation curves of P4G11 and P4G13 aptamers as examples. However, the $K_D$ determined by this fluorescence assay showed significant variation (40% standard deviation from the average $K_D$ value in some cases). Therefore, affinity binding was also attempted by the EIS method. A gold electrode surface was used as the solid support on which the P4 analyte was immobilized, as shown in the schematic diagram in Supporting Information (Figures S1 and S2). The progesterone molecules were immobilized on the Au electrode via the carboxylic groups, to keep the exposed site of the P4 molecules to DNA similar to that used in the selection step. The immobilization of P4 on the functionalized gold electrode was characterized by CV and EIS (Supporting Information, Figure S3, panels a and b, respectively). After the P4-modified electrodes were incubated with different concentration of the aptamer, we observed a remarkable increase in $R_{ct}$ due to binding with the negatively charged DNA, which retarded electron transfer of $[Fe(CN)_6]^{3-/4-}$ to the gold electrode (Supporting Information, Figure S4). The change in $R_{ct}$ was monitored and a saturation curve was plotted as shown in Figure 2b. As observed in Table 1, the $K_D$ values determined by EIS were close to the fluorescence method, which confirms the high affinity of the selected aptamers. Moreover, variation of the $K_D$ values determined by EIS was less than for the fluorescence assay as indicated by the lower standard deviation, which confirms the usefulness of the developed electrochemical binding affinity assay. A control measurement was also carried out by incubating the Au electrode with nonspecific DNA sequence. The low signal response to the nonspecific sequence indicated the selectivity of the EIS method (Figure 2b, black line).


DOI: 10.1021/ac503639s
Anal. Chem. 2015, 87, 1075−1082

**Scheme 2. Impedimetric Mechanism of Aptasensor**

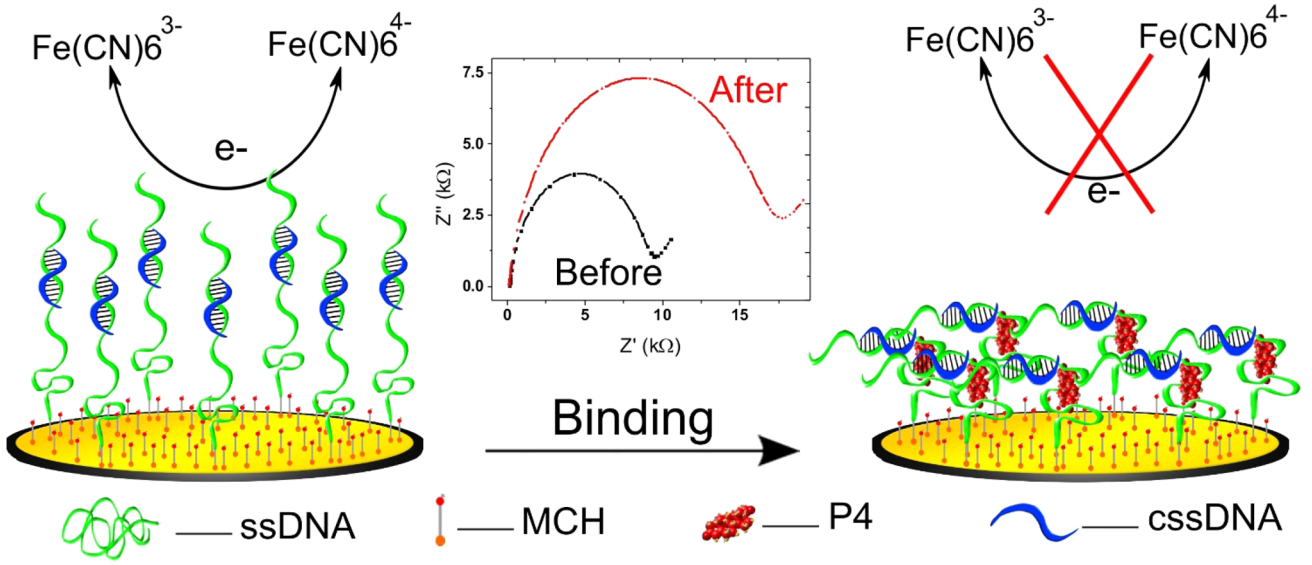


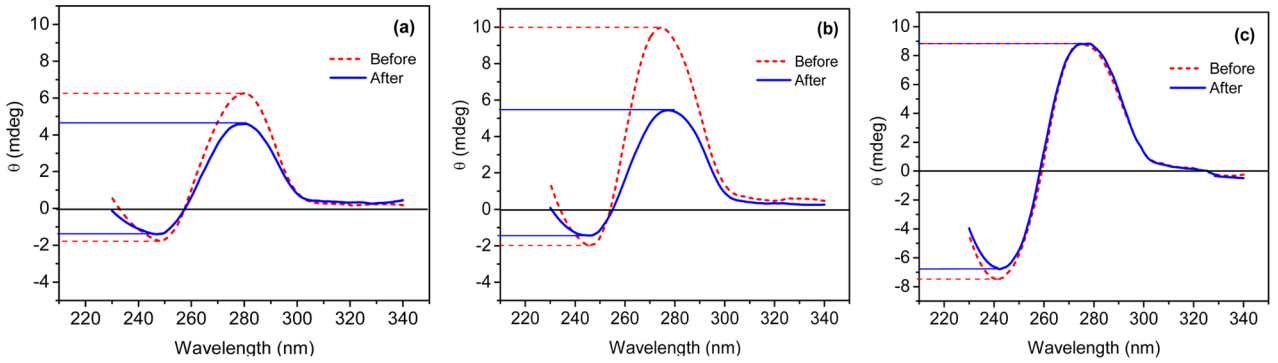


**Figure 4.** CD spectra of different aptameric arrangements before and after binding to 1.5 $\mu$M P4 analyte: (a) pure ssDNA P4G13 aptamer, (b) P4G13−cDNA2, or (c) P4G13−cDNA2 with 1.5 $\mu$M bisphenol A in binding buffer at 25 °C as a negative control. DNA samples were individually scanned from 340 to 230 nm at 100 nm/s scan rate.

Because our goal was to apply the selected aptamers in a label-free detection platform, it was important to study the conformational change of the aptamers with the highest affinity to progesterone (P4G03, P4G06, P4G11, and P4G13) before and after binding, by circular dichroism spectroscopy. As shown in Supporting Information Figure S5, the preliminary CD results showed that the aptamer P4G13 yielded more conformational change upon binding to P4 analyte.

To study the specificity of P4G13 aptamer, cross-reactivity assays with NET and E2, hormones that can present in the same environmental samples and have similar chemical structure, were performed by fluorescence assay. A very low DNA recovery percentage was obtained with NET− and E2−beads compared with the P4−beads (Figure 2c), which indicates the specificity of this aptamer.

**Electrochemical Aptasensor of Progesterone Detection.** Because of its high affinity and specificity, P4G13 aptamer was chosen to be utilized as a sensing probe in an electrochemical biosensing platform. First, the aptasensor was fabricated by immobilizing the disulfide-modified aptamer on the gold electrodes via self-assembly and characterized by CV as well as EIS. As shown in Figure 3a, a significant decrease in the anodic and cathodic peak currents of the $[Fe(CN)_6]^{3-/4-}$ redox couple with an increase in the peak separation ($\Delta E$) compared to the bare gold electrode was observed due to the negative charge of the DNA. Likewise, the charge-transfer resistance of $[Fe(CN)_6]^{3-/4-}$ to the gold electrode was increased after aptamer immobilization (Figure 3b), confirming the success of the self-assembly. The binding of P4 to the aptasensor resulted in a further small increase in $R_{ct}$. We presume that this change in $R_{ct}$ is not due to a blocking effect of such a small and neutral molecule (314.4 Da). However, we attribute this increase in the EIS signal to a partial change of the aptamer conformation upon binding to P4, causing more retardation of $[Fe(CN)_6]^{3-/4-}$ anions to the electrode surface and thus increasing the $R_{ct}$. The percentage change in charge-transfer resistance, $(R - R_0)/R_0$, between the signal of the blank and the P4 solution before reaching the saturation point was 17.6% with a calculated detection limit of 3.2 ng/mL, suggesting a poor response of the aptasensor to the P4 analyte (see Figure 3c and Supporting Information, Figure S6). With the aim to improve the response of the biosensing platform, different aptameric arrangements were tested to increase the conformational change of the aptamer after binding to the analyte. The design was based on partial hybridization of a short moiety of the aptamer with a complementary ssDNA fragment. Hence, five complementary ssDNA sequences (cDNA, 10-mer) of P4G13 at different sites were separately hybridized to the disulfide-


DOI: 10.1021/ac503639s
Anal. Chem. 2015, 87, 1075−1082

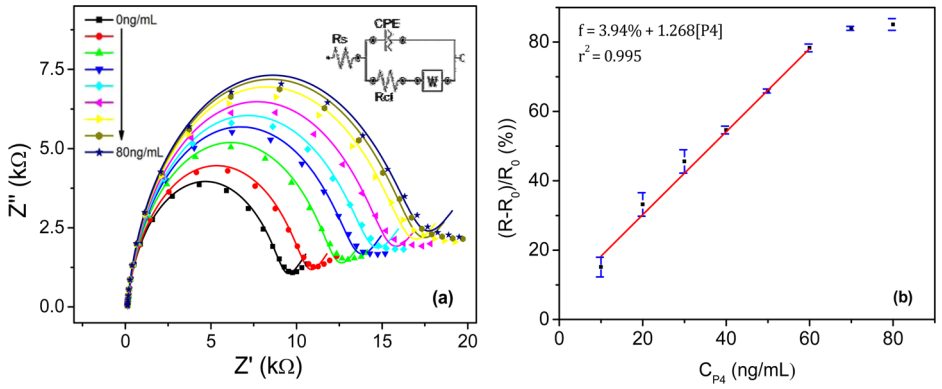


**Figure 5.** (a) Nyquist plots (EIS spectra) of faradaic measurements in 5 mM $[Fe(CN)_6]^{4-/3-}$ of the aptasensor in different concentrations of P4 analyte (0, 10, 20, 30, 40, 50, 60, 70, and 80 ng/mL); symbols correspond to the experimental data and lines to the fitted data. Each measurement was swept from 10 kHz to 0.1 Hz at a bias potential of 0.230 V with an alternating potential of 10 mV. (b) Calibration curve of the aptasensor; linear plot with regression coefficient $r^2$ = 0.995. The LOD was estimated to be 0.90 ng/mL with a linear range from 10 to 60 ng/mL.

modified P4G13 sequence (60-mer) and subsequently immobilized on the gold electrode. Figure 3c shows the response of the resultant pdsDNA aptasensors after incubation with the P4 analyte. It was observed that the resultant aptamer hybridized with the second complementary sequence (P4G13−cDNA2, 5′-TGGGCGGTGG-3′) showed the highest response after binding to the P4 analyte.

We believe that by hybridizing a moiety of the aptamer, we force the aptamer to adopt a different conformation that eventually will change in a distinct way by binding the analyte. This change has led to more significant blocking of the electron transfer, and in turn the $R_{ct}$ was increased (Scheme 2). On the other hand, the response of some of the tested P4G13−cDNA at other sites was even lower than that of the pure aptamer. This could be due to different conformation changes of the pdsDNA, which resulted in more access of the $[Fe(CN)_6]^{3-/4-}$ to the gold electrode. Moreover, possible displacement of the 10-mer cDNA that was hybridized to the binding site of the analyte with free progesterone may occur. The liberated cDNA can decrease the total negative charge on the electrode surface, leading to a decrease in $R_{ct}$. No signficant change was reported in the P4G13−cDNA2 sensor response after incubation with Bisphenol A, one water contaminant with 446 MW = 228.29 Da as a control, which indicate the specificity of the aptasensor. Figure 4 shows more significant change in the CD spectrum of P4G13−cDNA2 than of the pure aptamer upon binding with progesterone, whereas no change was observed with bisphenol A, which also supports our explanation. Figure 5a shows the P4G13−cDNA2 aptasensor upon binding with different concentrations of P4. An increase in the aptasensor response was observed in the range 10−60 ng/mL. A calibration plot is shown in Figure 5b that can be represented by the equation $(R - R_0)/R_0$ = 3.94% + 1.268[P4], with a detection limit (DL) of 0.90 ng/mL calculated as DL= $3S/b$, where S is the standard deviation of the blank and $b$ is the slope of the straight line. The standard deviations of the measurement ranged from 1% to 7%, indicating good reproducibility of the P4 aptasensor. This detection limit is comparable to the detection limits of some other reported electrochemical immunosensors.[16−18] Moreover, on the basis of these data, the affinity of the aptamer was again assessed by calculating the $K_D$ in the aptasensor configuration (Supporting Information, Figure S7). A value of 111.74 ± 24.58 nM was obtained, which is close to that previously obtained by fluorescence and EIS measurements (low nanomolar range). These results indicate that hybridization of the aptamer with the short complementary sequence and further anchoring to the gold surface did not significantly influence the affinity of the aptamer.

**Real Biosensing Application.** Spiked progesterone concentrations in tap water were tested to check the possibility of applying the developed EIS aptasensor in real samples. Good recovery percentages were obtained that indicate nonsignificant interference from the tap water components on the aptasensor detection. Hence, these results ratify the real application of the EIS aptasensor in environmental analysis (see Table S2 in Supporting Information).

## CONCLUSIONS

In this work, the selection and characterization of the first DNA aptamers with high affinity for progesterone was presented. Aptamer P4G13 ($K_D$ = 17 nM) showed excellent specificity to progesterone with no detectable cross-reactivity with its similar congeners E2 and NET. We showed by circular dichroism analysis that the conformation change of the aptamer upon binding with P4 was more significant when the aptamer was hybridized with a 10-mer short complementary sequence. This phenomenon has been exploited to develop a label-free aptasensor with enhanced signal gain monitored by EIS. The proposed aptasensor showed a linear dynamic range from 10 to 60 ng/mL with a limit of detection of 0.90 ng/mL. A preliminary application of the EIS aptasensor in spiked tap water samples showed a good recovery percentage. Application of the developed aptasensor in clinical samples will be studied in the future, as well as therapeutic biosensing applications of the selected progesterone aptamers.

## ASSOCIATED CONTENT

### Supporting Information

Additional text, seven figures, and two tables describing materials, reagents and instrumentation; in vitro selection of progesterone aptamers; cloning and sequencing of selected aptamers; immobilization of progesterone and electrografting of aryldiazonium salt on gold electrodes; characterization of gold electrode modification and immobilization of progesterone; binding affinity determination by EIS; CD studies of aptamer sequences; electrochemical aptasensor application of pure P4G13 aptamer for P4 detection, $K_D$ determination by aptasensor; and trials of spiked progesterone concentration



DOI: 10.1021/ac503639s
Anal. Chem. 2015, 87, 1075−1082

using the EIS aptasensor. This material is available free of charge via the Internet at http://pubs.acs.org.

## AUTHOR INFORMATION


### Corresponding Author

*E-mail siaj.mohamed@uqam.ca; tel +1514 987 3000, ext 1921.


### Notes

The authors declare no competing financial interest.

## ACKNOWLEDGMENTS

This work was made possible by support from the Natural Science and Engineering Research Council of Canada (NSERC) and Le Fonds de Recherche du Québec—Nature et Technologies (FQRNT). We gratefully acknowledge the fellowship received by G.C.J. from the FQRNT scholarship program for international students. We acknowledge all the characterization centers including NanoQAM, Le Centre de Caractérisation Microscopique des Matériaux ($CM^2$), and CoFaMic. We thank Professor Mario Morin for valuable help for LMFE laboratory renovation.

## REFERENCES


(1) Diamanti-Kandarakis, E.; Bourguignon, J. P.; Giudice, L. C.; Hauser, R.; Prins, G. S.; Soto, A. M.; Zoeller, R. T.; Gore, A. C. *Endocr. Rev.* **2009**, *30*, 293−342.

(2) Hewitt, J. K.; Campbell, P.; Porpavai, K.; Grover, S. R.; Newman, L. K.; Warne, G. L. *Med. J. Aust.* **2012**, *196* (9), 578−581.

(3) King, T. L.; Brucker, M. C. *Pharmacology for Women's Health*, 1st ed.; Jones & Bartlett Publishers: San Francisco, CA, 2010; p 372.

(4) Sherwin, B. B. *J. Reprod. Med.* **1999**, *44* (Suppl 2), 227−232.

(5) Ganmaa, D.; Sato, A. *Med. Hypotheses* **2005**, *65*, 1028−1037.

(6) Kanasaki, H.; Purwana, I. N.; Mijiddorj, T.; Sukhbaatar, U.; Oride, A.; Miyazaki, K. *Neuro Endocrinol. Lett.* **2012**, *33*, 608−613.

(7) Schneider, J. S.; Stone, M. K.; Wynne-Edwards, K. E.; Horton, T. H.; Lydon, J.; O'Malley, B.; Levine, J. E. *Proc. Natl. Acad. Sci. U.S.A.* **2003**, *100*, 2951−2956.

(8) Beiraghi, A.; Pourghazi, K.; Amoli-Diva, M. *Anal. Methods* **2014**, *6*, 1418−1426.

(9) Tolgyesi, A.; Verebey, Z.; Sharma, V. K.; Kovacsics, L.; Fekete, J. *Chemosphere* **2010**, *78*, 972−979.

(10) Capparelli, R.; Iannelli, D.; Bordi, A. *J. Dairy Res.* **1987**, *54*, 471−477.

(11) Shrivastav, T. G.; Chaube, S. K.; Charu; Rangari, K.; Kariya, K. P.; Singh, R.; Nagendra, A. *J. Immunoassay Immunochem.* **2010**, *31*, 301−313.

(12) Gillis, E. H.; Traynor, I.; Gosling, J. P.; Kane, M. *J. AOAC Int.* **2006**, *89*, 838−842.

(13) Tschmelak, J.; Kappel, N.; Gauglitz, G. *Anal. Bioanal. Chem.* **2005**, *382*, 1895−903.

(14) Kappel, N. D.; Proll, F.; Gauglitz, G. *Biosens. Bioelectron.* **2007**, *22*, 2295−2300.

(15) Ehrentreich-Forster, E.; Scheller, F. W.; Bier, F. F. *Biosens. Bioelectron.* **2003**, *18*, 375−380.

(16) Carralero, V.; González-Cortés, A.; Yáñez-Sedeño, P.; Pingarrón, J. M. *Anal. Chim. Acta* **2007**, *596*, 86−91.

(17) Pemberton, R. M.; Hart, J. P.; Mottram, T. T. *Biosens. Bioelectron.* **2001**, *16*, 715−723.

(18) Kreuzer, M. P.; McCarthy, R.; Pravda, M.; Guilbault, G. G. *Anal. Lett.* **2005**, *37*, 943−956.

(19) Arevalo, F. J.; Messina, G. A.; Molina, P. G.; Zon, M. A.; Raba, J.; Fernandez, H. *Talanta* **2010**, *80*, 1986−1992.

(20) National Health and Medical Research Council. *Australian code for the care and use of animals for scientific purposes*, 2013.

(21) Perry, M. *Aust. Vet. J.* **1998**, *76*, 286.

(22) Ellington, A. D.; Szostak, J. W. *Nature* **1990**, *346*, 818−822.

(23) Tuerk, C.; Gold, L. *Science* **1990**, *249*, 505−510.

(24) Stoltenburg, R.; Reinemann, C.; Strehlitz, B. *Biomol. Eng.* **2007**, *24*, 381−403.

(25) Stoltenburg, R.; Reinemann, C.; Strehlitz, B. *Anal. Bioanal. Chem.* **2005**, *383*, 83−91.

(26) Liang, H. R.; Hu, G. Q.; Xue, X. H.; Li, L.; Zheng, X. X.; Gao, Y. W.; Yang, S. T.; Xia, X. Z. *Virus Res.* **2014**, *184*, 7−13.

(27) Umekage, S.; Kikuchi, Y. *Nucleic Acids Symp. Ser. (Oxford)* **2006**, 323−324.

(28) Mann, D.; Reinemann, C.; Stoltenburg, R.; Strehlitz, B. *Biochem. Biophys. Res. Commun.* **2005**, *338*, 1928−1934.

(29) Reinemann, C.; Stoltenburg, R.; Strehlitz, B. *Anal. Chem.* **2009**, *81*, 3973−3978.

(30) Ng, A.; Chinnappan, R.; Eissa, S.; Liu, H.; Tlili, C.; Zourob, M. *Environ. Sci. Technol.* **2012**, *46*, 10697−10703.

(31) Eissa, S.; Ng, A.; Siaj, M.; Tavares, A. C.; Zourob, M. *Anal. Chem.* **2013**, *85*, 11794−11801.

(32) Gao, C.; Wang, Q.; Gao, F. *Chem. Commun.* **2014**, *50*, 9397−9400.

(33) Kim, Y. S.; Jung, H. S.; Matsuura, T.; Lee, H. Y.; Kawai, T.; Gu, M. B. *Biosens. Bioelectron.* **2007**, *22*, 2525−2531.

(34) Grozio, A.; Gonzalez, V. M.; Millo, E.; Sturla, L.; Vigliarolo, T.; Bagnasco, L.; Guida, L.; D'Arrigo, C.; De Flora, A.; Salis, A.; Martin, E. M.; Bellotti, M.; Zocchi, E. *Nucleic Acid Ther.* **2013**, *23*, 322−331.

(35) Kawazoe, N.; Ito, Y.; Shirakawa, M.; Imanishi, Y. *Bull. Chem. Soc. Jpn.* **1998**, *71*, 1699−1703.

(36) Williams, K. P.; Liu, X. H.; Schumacher, T. N. M.; Lin, H. Y.; Ausiello, D. A.; Kim, P. S.; Bartel, D. P. *Proc. Natl. Acad. Sci. U.S.A.* **1997**, *94*, 11285−11290.

(37) Fischer, L. M.; Tenje, M.; Heiskanen, A. R.; Masuda, N.; Castillo, J.; Bentien, A.; Émneus, J.; Jakobsen, M. H.; Boisen, A. *Microelectron. Eng.* **2009**, *86*, 1282−1285.

(38) Haskins, A. L. *Exp. Biol. Med.* **1949**, *70*, 228−229.




DOI: 10.1021/ac503639s
*Anal. Chem.* 2015, 87, 1075−1082